DOI: 10.1534/genetics.105.043265

Drosophila *starvin* Encodes a Tissue-Specific BAG-Domain Protein Required for Larval Food Uptake

Michelle Coulson,* Stanley Robert*,[1] and Robert Saint*,†,[2]

**ARC Special Research Centre for the Molecular Genetics of Development, School of Molecular and Biomedical Sciences, University of Adelaide, Adelaide, South Australia 5005, Australia and* †*Research School of Biological Sciences, Australian National University, Canberra City, ACT 2601, Australia*

Manuscript received March 14, 2005
Accepted for publication August 25, 2005

ABSTRACT

We describe a developmental, genetic, and molecular analysis of the sole Drosophila member of the BAG family of genes, which is implicated in stress response and survival in mammalian cells. We show that the gene, termed *starvin* (*stv*), is expressed in a highly tissue-specific manner, accumulating primarily in tendon cells following germ-band retraction and later in somatic muscles and the esophagus during embryonic stage 15. We show that *stv* expression falls within known tendon and muscle cell transcriptional regulatory cascades, being downstream of *stripe*, but not of another tendon transcriptional regulator, *delilah*, and downstream of the muscle regulator, *mef-2*. We generated a series of *stv* alleles and, surprisingly, given the muscle and tendon-specific embryonic expression of *stv*, found that the gross morphology and function of somatic muscles is normal in *stv* mutants. Nonetheless, *stv* mutant larvae exhibit a striking and fully penetrant mutant phenotype of failure to grow after hatching and a severely impaired ability to take up food. Our study provides the first report of an essential, developmentally regulated BAG-family gene.

MAMMALIAN Bcl1-associated athanogene (BAG)-domain proteins, named after the founding member BAG-1 (Takayama *et al.* 1995), are Hsp70-family cochaperones implicated in cell survival, intracellular signaling, gene expression, and human disorders such as Parkinson's disease (Takayama *et al.* 1995, 1997, 1999; Gebauer *et al.* 1997; Höhfeld and Jentsch 1997; Zeiner *et al.* 1997; Liu *et al.* 1998; Antoku *et al.* 2001; Briknarova *et al.* 2002; Kalia *et al.* 2004; reviewed in Doong *et al.* 2002; Alberti *et al.* 2003; Gehring 2004; Townsend *et al.* 2005). The ~80-amino-acid C-terminal BAG domain comprises an antiparallel, amphipathic, three-helix bundle structure (Briknarova *et al.* 2001; Sondermann *et al.* 2001; Brockmann *et al.* 2004; Symersky *et al.* 2004), which interacts with the ATPase domain of Hsc70 and Hsp70 (Höhfeld and Jentsch 1997; Takayama *et al.* 1997). BAG-domain proteins can act as nucleotide exchange factors that influence cycling between ADP-bound and ATP-bound forms, directly regulating the activity of HSP70 and HSC70 (Höhfeld and Jentsch 1997; Höhfeld 1998; Gassler *et al.* 2001). BAG-domain proteins also form complexes with other proteins, such as Bcl-2 (Takayama *et al.* 1995; Antoku *et al.* 2001), Raf kinase (Wang *et al.* 1996; Song *et al.* 2001), steroid receptors (Froesch *et al.* 1998; Kullmann *et al.* 1998; Shatkina *et al.* 2003), tyrosine kinase receptors (Bardelli *et al.* 1996), the cellular stress response protein GADD34 (Hung *et al.* 2003), and Siah (Matsuzawa *et al.* 1998). Some of these interactions have been shown to be independent of Hsp70-family chaperones, potentially expanding the functions of this family of proteins beyond those of the cellular stress response, although Hsc70 and Hsp70 are the main binding partners of BAG-1 in cellular extracts (Höhfeld and Jentsch 1997; Takayama *et al.* 1997).

Six mammalian BAG-family members have been identified: BAG 1, BAG-2, BAG-3/CAIR-1, BAG-4/SODD, BAG-5, and HLA-B/BAT3, the human ortholog of Scythe (Takayama *et al.* 1999; Manchen and Hubberstey 2001).

Despite the broad significance of this family of proteins, BAG-family members are yet to be analyzed from a developmental or genetic perspective. Here we present a developmental and genetic analysis of a *Drosophila melanogaster* BAG-family gene that we have named *starvin* (*stv*). Surprisingly, we found *stv* expression to be regulated in a highly developmentally specific fashion, being expressed primarily in developing larval somatic muscles and their epidermal tendon (muscle attachment) cells and less strongly in the esophagus. This tissue-specific expression appears not to be required for gross muscle morphology, which showed no apparent disruption in *stv* mutant embryos. However, we show that *stv* is essential for viability, specifically for the

[1]*Present address:* CSIRO Marine Research, GPO Box 1538, Hobart TAS 7001, Australia.

[2]*Corresponding author:* Research School of Biological Sciences, Australian National University, GPO Box 475, Canberra City, ACT 2601, Australia. E-mail: robert.saint@anu.edu.au

ability of newly hatched larvae to ingest food and grow, indicating that subtle or nonmorphological muscle or esophageal-specific defects required for feeding are disrupted in *stv* mutant embryos.

MATERIALS AND METHODS

Drosophila stocks: *UAS::dei* was obtained from A. Michelson (Howard Hughes Medical Institute, Brigham and Women's Hospital, Boston); *UAS::sr^{138}* (third chromosome) was obtained from T. Volk (Weizmann Institute of Science, Rehovot, Israel); *69B Gal4/CyO* was obtained from M. Muskavitch (Indiana University, Bloomington, IN); β*3Tubulin::lacZ* was obtained from D. Buttgereit (Phillips-University Marburg, Marburg, Germany); *UAS::mef2* was obtained from B. Bour (Pennsylvania State University, University Park, PA); *en::Gal4* was obtained from A. Brand (University of Cambridge, Cambridge, UK). Other Drosophila stocks were obtained from the Bloomington (Indiana) stock center.

Antibodies: Rabbit anti-Alien antibody (Goubeaud *et al.* 1996) was obtained from A. Paululat (Phillips-University Marburg, Marburg, Germany). Rabbit anti-GFP was purchased from CLONTECH (Pala Alto, CA). Rabbit antimuscle myosin (Kiehart and Feghali 1986) was obtained from D. Kiehart (Duke University Medical School, Durham, NC). Other monoclonal antibodies used in this study were obtained from the Developmental Studies Hybridoma Bank under the auspices of the National Institute of Child Health and Human Development and maintained at the University of Iowa. Rabbit antibodies were raised against a Starvin (STV)-maltose binding protein (MBP) fusion protein and affinity purified first by passing the serum over a MBP column to deplete MBP-specific antibodies and then by passing the eluate over a STV::MBP column and eluting the bound fraction. Rat anti-STV antibodies were raised against a STV::GST fusion protein and affinity purified using a MBP::STV column. The secondary antibodies goat anti-rabbit biotin, donkey anti-rabbit HRP, donkey anti-rat biotin, goat anti-rat HRP, and donkey anti-mouse biotin were affinity purified polyclonals purchased from Jackson ImmunoResearch (West Grove, PA). The Vectastain ABC kit (Vector Laboratories, Burlingame, CA) was used to visualize the antibody stains.

Drosophila embryo whole-mount antibody staining: Embryos were collected from egg-laying chambers on grape juice agar plates partially spread with yeast paste. Eggs were collected, dechorionated by soaking in 50% bleach, then washed thoroughly in water or 7.5 mm Na_2HPO_4, 2.5 mm NaH_2PO_4, 145 mm NaCl, 1% Tween 20 (PBT). Embryos were fixed in 3.7% formaldehyde. Blocking (with either 5% Blotto or 2% goat serum) was performed for a minimum of 30 min. Embryos were incubated with primary antibody overnight at 4° with gentle agitation. After washing, embryos were incubated in secondary antibody for at least 1 hr at 25°, or overnight at 4°, and washed repeatedly before the color reaction was carried out using diaminobenzidine (DAB). If a blue/black staining was desired, rather than the default brown, the final DAB solution also contained a 0.08% $NiCl_2$. Embryos were rinsed four to eight times in PBT, followed by one 5-min wash before being placed under 80% glycerol in PBT for mounting.

***P*-element and EMS mutagenesis:** The *P*-element insertion line *l(3)00543* (FlyBase 1999) was obtained from the Bloomington *Drosophila* Stock Center. Imprecise excisions were achieved by crossing in a source of Δ2-3 transposase and selecting for loss of the *ry*$^+$ marker and for decreased viability when *trans*-heterozygous with *l(3)00543*. Chemical mutagenesis was performed on an isogenized *ru st e ca* strain. Male flies were fed ethyl methanesulfonate in a sucrose solution as described in Grigliatti (1986) and progeny were screened for lethality when *trans*-heterozygous with the excision deletion *Df(3L)stv3c*. Three lethal lines (*stv*^{1}, *stv*^{2}, and *stv*^{3}) and one semilethal line (*stv*^{4}) were obtained from 5000 mutagenized third chromosomes. To aid sequencing of alleles, interspecific hybrids were obtained by crossing *stv*$^-$*/TM3rySb D. melanogaster* females to *D. simulans* males (obtained from the Bloomington stock center) and selecting for non-Sb progeny as the source of DNA to be amplified using *melanogaster*-specific primers. All *stv* mutant phenotypic analyses were performed on maternal$^-$ zygotic$^-$ (m$^-$z$^-$) germline clone mutants produced following the method of Chou and Perrimon (1996).

Feeding ability assay: Larvae were separated into m$^-$z$^-$ and m$^-$z$^+$ classes on the basis of a GFP-marked balancer chromosome and placed onto a fresh grape agar plate, which contained yeast paste mixed with bromophenol blue, an indigestible dye that is visible in the alimentary system of the larva. Larvae were scored for feeding status every 12–24 hr, at which point they were transferred to a fresh indicator plate.

RESULTS

***starvin* encodes a BAG-domain protein:** Drosophila *stv* was isolated as a λ-phage expression plaque that bound radiolabeled Polycomblike (Pcl) protein using a previously described filet-based technique (Robert and Saint 1998). Subsequent extensive genetic interaction analysis (data not shown) and developmental and subcellular localization data (see below) indicated that this interaction was almost certainly artifactual. Nevertheless, we pursued the analysis of this gene because we found it to be a member of a family of genes that are postulated to play important roles in mammalian cells (see below), yet no member of this gene family had been subjected to genetic analysis. Sequence analysis of the cDNA revealed a 79-aa region in the carboxy terminal region of STV that shares sequence similarity with three known human proteins, BAG-3/CAIR-1, BAG-4, and BAG-5 (Figure 1A). The region of similarity between these BAG-family members and BAG-1, BAG-2, and HLA-B/BAT3/Scythe defines the BAG domain (Takayama *et al.* 1999; Thress *et al.* 2001). The region of recognizable similarity between STV and BAG-3, BAG-4, and the two BAG domains of BAG-5 extends beyond the BAG domain defined by Takayama *et al.* (1999), enlarging it to 79 aa (Figure 1A). STV has the highest sequence similarity over this region with BAG-4, a lower similarity with BAG-3 and BAG-5 (Figure 1A), and much less similarity to the BAG-1, BAG-2, and Scythe BAG domains (data not shown). BAG-1, BAG-2, and Scythe also have relatively low levels of similarity with all other BAG-family proteins. All BAG-family proteins identified so far, including STV, have a BAG domain close to the carboxyl terminus of the protein, although BAG-5 also has an amino-located BAG domain (Takayama *et al.* 1999). BLAST analysis of the amino acid sequence of BAG-domain proteins, including STV, failed to reveal any other members of this family in the *D. melanogaster* genome (results not shown).

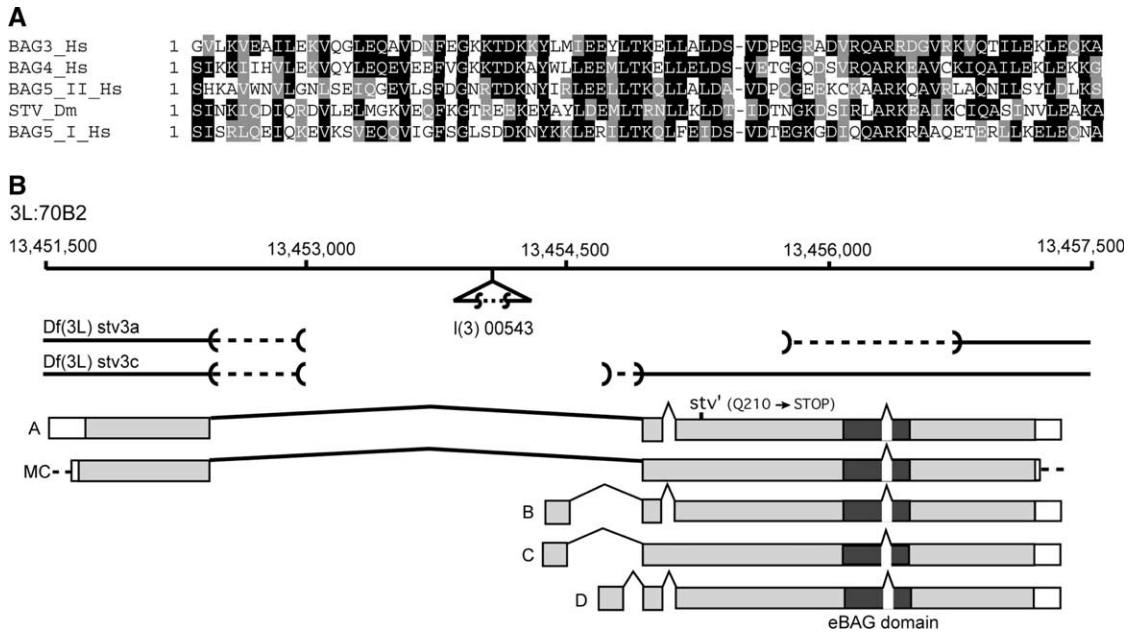

FIGURE 1.—(A) Alignments of selected BAG domains, showing identical (solid background) and similar (shaded background) residues. STV is most similar to the human BAG-4 protein, while BAG-1 and BAG-2 are the least similar of the five human BAG-family members. Dm, *D. melanogaster*; Hs, *Homo sapiens*. Accession nos: BAG-1 (*H. sapiens*) gpAAC34258; BAG-2 (*H. sapiens*) gpAAD16121; BAG-3 (*H. sapiens*) gpAAD16122; BAG-4 (*H. sapiens*) gpAAD16123; BAG-5 (*H. sapiens*) gpAAD16124. (B) The genomic region at 70B2 covering the *stv* locus and showing the intron-exon structure of the longest *stv* cDNA (labeled A) and the open reading frames (shaded) of this cDNA and three other open reading frames listed in FlyBase (labeled B, C, and D, respectively). In addition, a cDNA clone that we analyzed and that has a structure different from the FlyBase cDNA sequences is also represented (labeled MC). The location of the l(3)00543 *P* element is marked. The extent of two of the *P*-element-induced lethal deficiencies is shown, as is the position of the mutated codon in the stv^1 allele. The dashed lines indicate the region within which the breakpoints lie. The numbers indicate the genome sequence position along the third chromosome.

Sequence analysis revealed that *stv* corresponds to CG32130, a computer-annotated gene located at 70B2 on the left arm of the *D. melanogaster* third chromosome. Conceptual translation of a full-length cDNA (BROWN and KAFATOS 1988) revealed a 635-amino-acid, 69-kDa protein with an exon structure different from those derived from the Drosophila genome project analyses (Figure 1B). In addition to the BAG domain, another prominent feature of STV is the relative abundance of glutamine, proline, and alanine residues, which make up 38% of the amino acid content (data not shown), although they are particularly sparse over the BAG-domain region.

***starvin* is expressed specifically in embryonic somatic muscle and tendon cells:** To determine the subcellular localization and tissue distribution of STV, rabbit and rat antibodies were raised against bacterially expressed STV fusion proteins (see MATERIALS AND METHODS). Staining of whole-mount embryos showed that STV is not expressed prior to the completion of germ-band retraction (data not shown) but is first detected in a small number of cells during the early stages of dorsal closure (Figure 2A). STV becomes more widely distributed as embryogenesis proceeds (Figure 2, B and C), with faint stripes of expression appearing and increasing in intensity as dorsal closure progresses. These stripes correspond to tendon (muscle attachment) cells at the segmental boundaries. During dorsal closure, in addition to the stripes, various small clusters of cells expressing STV between the stripes were observed, and a somewhat more general staining developed laterally (Figure 2, D and E). The nature of these clusters has not been determined. It is likely that they represent cells that will become the attachment points for the lateral transverse muscles and other muscles that do not attach at the segment border. The tendon-specific transcription factor, Stripe, localizes during stage 13 in similar intrasegmental clusters, which later refine to become the attachment sites of muscles LT1–3 (LEE *et al.* 1995; FROMMER *et al.* 1996). The bulk of the remaining intrasegmental staining is due to the presence of STV in the somatic muscles (see below). By stage 15, the embryonic pattern of STV localization is essentially mature (Figure 2F).

***starvin* is expressed in tendon cells that attach body wall and head muscles:** Similarities between the pattern of expression of STV and the published expression patterns of other genes suggested that STV is present in epidermal tendon cells. To confirm this, we directly compared the dorsal, lateral, and ventral aspects of STV localization with genes known to be expressed in epidermal tendon cells. STV has a very distinctive dorsal

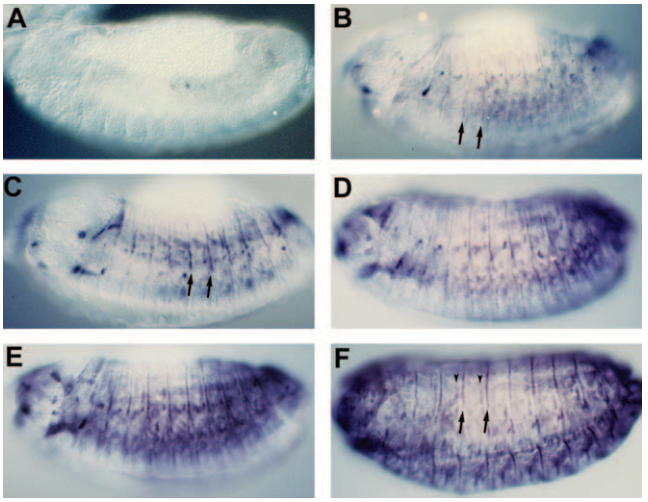

FIGURE 2.—Developmental profile of *stv* embryonic expression revealed by whole-mount anti-STV staining. All views are lateral. (A) A stage 13 embryo showing the earliest detectable STV expression, after germ-band retraction has been completed. (B) A mid-stage 13 embryo. STV localization is much more extensive, although very faint compared with older embryos. Intersegmental stripes (arrows) can be seen, in addition to spots of localization. (C) A late stage 13 embryo. Staining is darker, especially in the intersegmental stripes (arrows), and the level of intrasegmental staining is increasing. (D and E) Early and late stage 14 embryos. (F) The mature embryonic STV expression pattern at stage 15. This corresponds to the stage at which most muscles have formed their attachments with the epidermis. STV is present in intersegmental (arrows) and intrasegmental (arrowheads) attachment cells and in muscles.

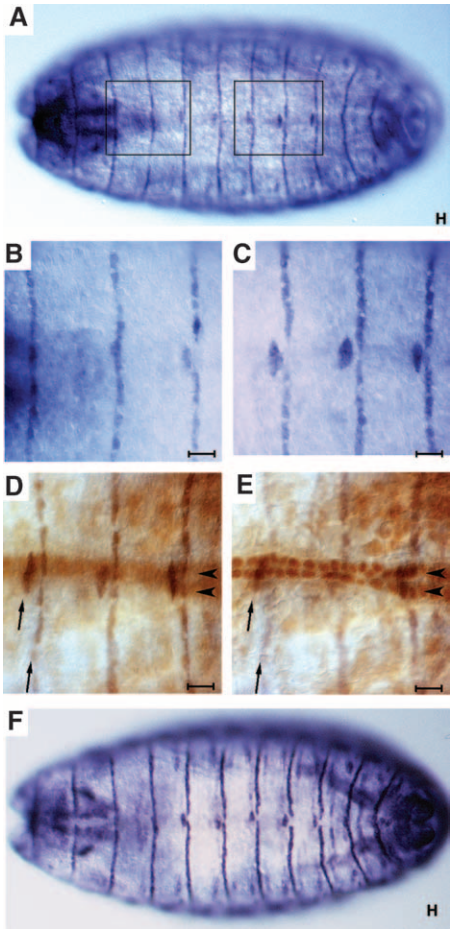

FIGURE 3.—STV is present in all dorsal epidermal tendon cells. All panels are dorsal views of stage 16 embryos. (A) Anti-STV staining reveals one stripe of STV per segment, extending across the dorsal epidermis of the embryo. Five of these stripes, those at the anterior of segments A2–A6, are broken at the dorsal midline. (B) Higher magnification of the anterior segments boxed in A showing stripes anterior to segments T3, A1, and A2. Only that of A2 is broken at the dorsal midline. (C) Higher magnification of the posterior segments boxed in A showing three stripes of STV localization which are all broken at the dorsal midline (anterior of segments A4–A6). (D) A higher-magnification view of a *how*$^{E7\text{-}3\text{-}4\ lacZ}$ embryo, an enhancer trap that expresses strongly in nuclei of dorsal vessel cells that flank the dorsal midline. The darker staining in focus shows STV expression (arrows) while the lighter brown color is anti-βGal staining of the dorsal vessel nuclei (arrowheads, out of focal plane). (E) The same embryo with the dorsal vessel nuclei staining in focus and STV staining out of focus. The STV stripes have a width of one cell and the broken portion of the stripe represents two cells, one on either side of the dorsal midline, which are displaced one cell from the main stripe. (F) Anti-Alien staining, showing the same pattern as STV localization. Alien is present in epidermal tendon cells (GOUBEAUD *et al.* 1996). All bars, 10 μm.

expression pattern of stripes at the segment boundary (Figure 3A). In segments A2–A6 these stripes are disrupted at the dorsal midline, and there is additional localization in clusters of cells anterior to the main stripe (Figure 3, A–C). Double immunostainings using an enhancer trap that expresses in the dorsal vessel confirmed that both aspects of dorsal STV localization are epidermal (Figure 3, D and E). Each displaced cell cluster at the dorsal midline consists of two cells, one per hemi-segment, which are shifted one cell to the anterior of the main stripe. These cells function as attachment cells for a fragment of muscle DA1, which splits into two at its posterior end and forms two attachments at the dorsal midline (ARMAND *et al.* 1994). The dorsal aspects of STV localization are identical to those of Alien (Figure 3F), a known marker of epidermal tendon cells (GOUBEAUD *et al.* 1996), confirming that STV is present in these cells.

The lateral localization of STV was found to be more complex than its dorsal localization (Figure 4), a reflection of the diversity of muscles in the lateral region. The three major regions of attachment cells were all found to express *stv* (groups I, II, and III of ARMAND *et al.* 1994; Figure 4A). These regions represent cells that form attachments with multiple muscles. STV was also detected in the attachment cells for the lateral transverse muscles, but staining was not clearly seen in most other cells that form attachments with single muscles (Figure 4A). However, in this regard STV behaves in the same manner as Kakapo, Alien, and

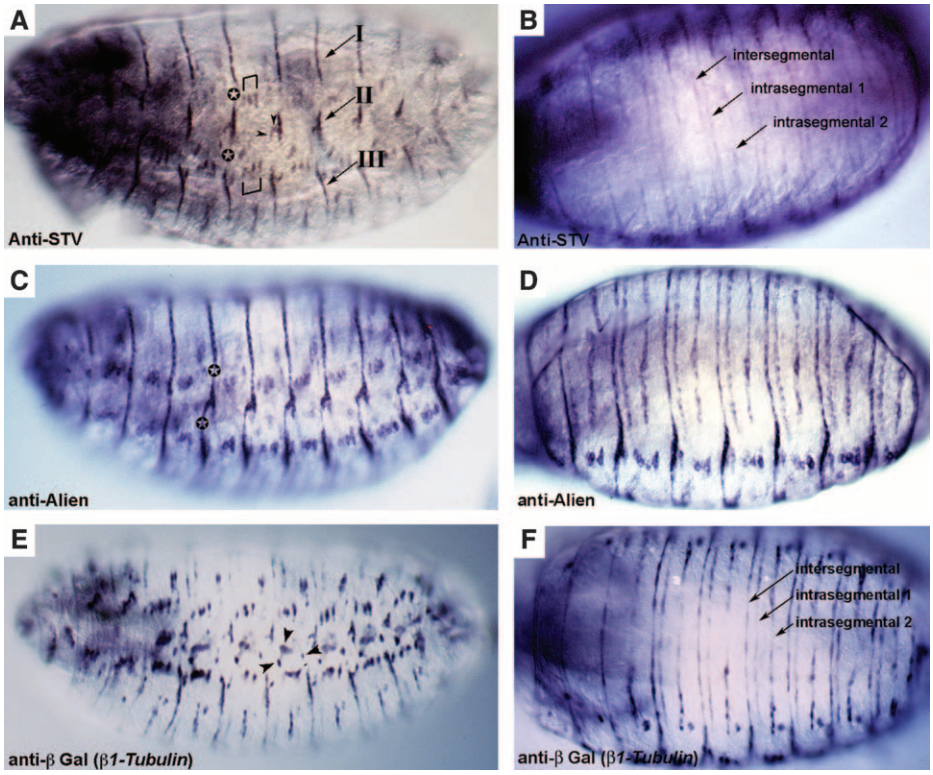

FIGURE 4.—STV is present in lateral epidermal and ventral epidermal tendon cells. All embryos are at stage 16. (A, C, and E) Lateral views. (B, D, and F) Ventral views. (A and B) Anti-STV staining. (A) The stripes of STV localization that are observed dorsally (Figure 3) are disrupted laterally. The dorsal stripes form attachment group I. STV is also present in the short lateral stripe representing group II and the more ventral group III. Brackets mark the dorsal and ventral attachments of muscles LT1 (21), LT2 (22), and LT3 (23). Arrowheads indicate the ventral attachment of muscle DT1 (18) and the posterior attachment of muscle DO5 (20). Other single attachment points cannot be readily identified. (B) Three stripes of STV localization per segment are observed ventrally. Morphologically, these stripes will generate three furrows, or apodemes: one intersegmental and two intrasegmental (CAMPOS-ORTEGA and HARTENSTEIN 1997). (C and D) Anti-Alien staining. (C) Alien expression differs from STV expression by continuing across the lateral regions among the attachment groups I, II, and III (indicated by a star). (D) A ventral view shows a pattern identical to that of STV. (E and F) Anti-βGal staining of an embryo carrying a β*1Tubulin::lacZ* construct. (E) *lacZ* is expressed in all tendon cells plus the chordotonal organs (arrowheads). Like STV, β1Tubulin expression is absent among the attachment groups. (F) β1Tubulin is expressed in the same three stripes per segment as STV and Alien.

β1Tubulin (Alien and β1Tubulin shown in Figure 4, C and E, respectively; BUTTGEREIT 1996; GOUBEAUD *et al.* 1996; STRUMPF and VOLK 1998).

The pattern of STV localization in the ventral region of the embryo is also representative of genes known to be expressed in epidermal tendon cells (Figure 4, B, D, and F). Three stripes of STV localization were observed in each abdominal segment (Figure 4B), the same pattern seen for β1Tubulin and Alien (Figure 4, D and F; BUTTGEREIT 1996; GOUBEAUD *et al.* 1996). The three stripes represent the intersegmental and two intrasegmental apodemes (the morphological indentation produced by tendon cell differentiation and muscle attachment), the intrasegmental apodemes being present only at the ventral surface of the embryo (CAMPOS-ORTEGA and HARTENSTEIN 1997). The presence of three apodemes is a consequence of muscles attaching at three different points per segment. Localization of all markers of epidermal tendon cells continues along the portion of the apodemes where muscles are not attached, in contrast to the lateral gaps in staining (see above).

We also observed strong STV expression in the head (Figure 5). The most prominent muscle group of the head is the dorsal pharyngeal musculature (DPM), which is formed from numerous fibers that run dorsoventrally. Dorsally, the DPM attaches at the ventral plane of the dorsal pouch. The ventral attachments are at the dorsal pharyngeal epithelium (CAMPOS-ORTEGA and HARTENSTEIN 1997). STV was observed in two broad rows of cells in a manner identical to Alien, Stripe, and β1Tubulin, which identifies these cells as the dorsal attachment cells of the DPM (Figure 5, A–D). Visualizing the distinctive morphology of the DPM showed that the attachment cells, rather than the musculature itself, were stained (Figure 5, E–L). STV and Alien are present in the dorsal attachments of the DPM only, while Stripe and β1Tubulin are localized to both dorsal and ventral attachments (Figure 5, I–L). GOUBEAUD *et al.* (1996) showed the presence of Alien in the DPM ventral attachments, but we saw no such localization (compare Figure 5J with K and L and Figure 5N with O and P). It is possible that Alien is present in the ventral attachments at a lower concentration than in the dorsal attachment, although the clear lateral view of both sets of attachments shows strong staining dorsally, but no detectable staining ventrally. From the ventral side of the embryo the ventral attachments can be discerned as an alignment of two rows of cells, as observed for Stripe and β1Tubulin, but not for STV and Alien (Figure 5, M–P).

In addition to attachment cells of the DPM, STV is localized in the head to a cluster of cells either side of the DPM, as is Alien, Stripe, and β1Tubulin (Figure 5, A–D). These cells are tendon cells that attach to other

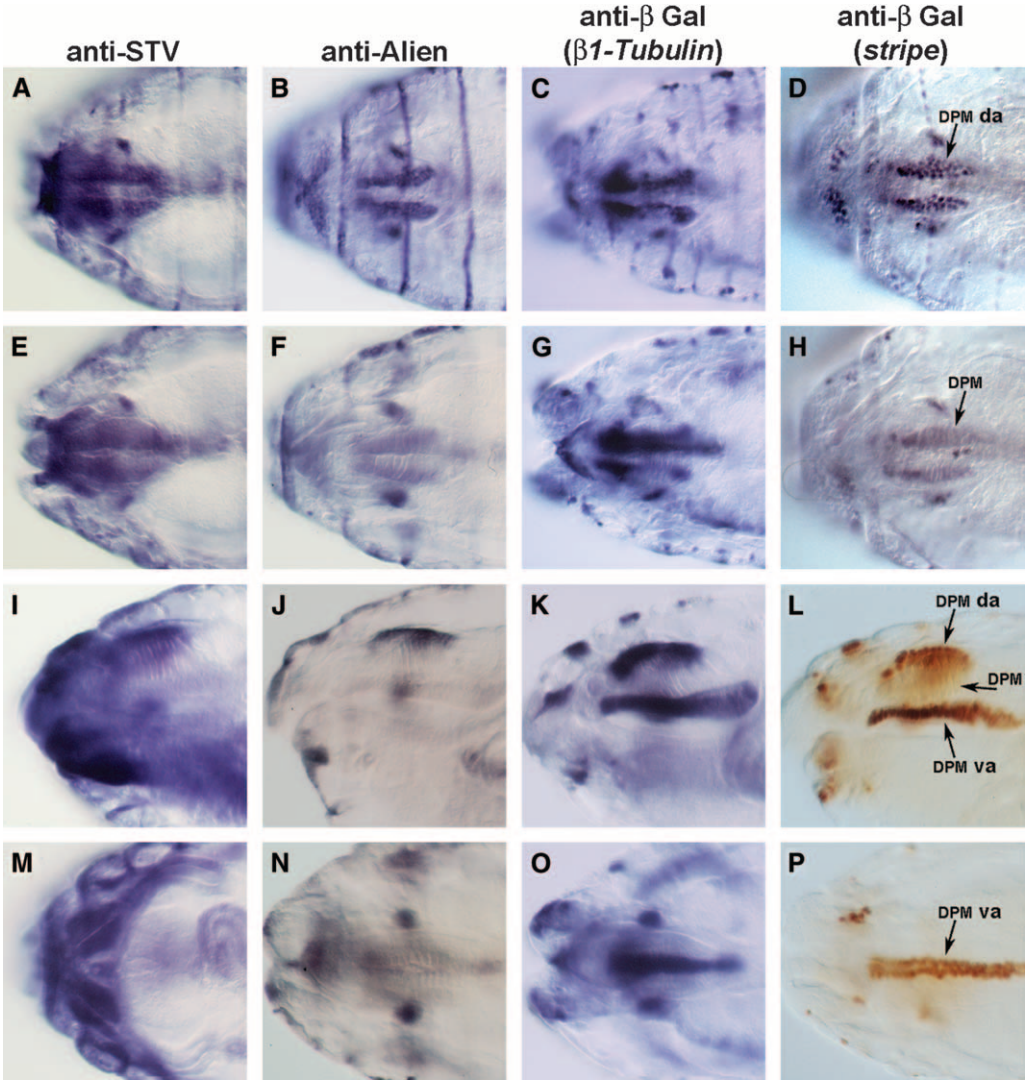

FIGURE 5.—The pattern of STV expression in the stage 16 embryonic head. A, E, I, and M are stained with anti-STV. B, F, J, and N are stained with anti-Alien. (C, G, K, and O) Embryos carrying a β*1Tubulin::lacZ* promoter construct stained with anti-β̃galactosidase. (D, H, L, and P) Embryos carrying an enhancer trap inserted in *stripe* and stained with anti-β-galactosidase. (A–H) Dorsal views. (A) STV is present in the dorsal attachment of the DPM. STV is expressed in essentially the same pattern as Alien, β1Tubulin, and Stripe markers (B–D), confirming that STV is expressed in tendon cells. (E–H) The same embryos shown in A–E viewed in a different focal plane, focused on the DPM, showing staining for STV to be out of focus and confirming that STV is present in the attachment cells of the DPM. (I–L) Lateral views. (I) STV is localized to the dorsal attachments of the DPM, but not to the DPM itself. The ventral attachment cells of the DPM did not stain. (J–L) Alien, β1Tubulin, and Stripe expression, respectively. Dorsal attachment but not ventral attachment localization is evident for Alien, while β1Tubulin and Stripe are present in both dorsal and ventral attachments of the DPM. (M–P) Ventral views. STV is expressed strongly in the large ventral intersegmental muscles (VIS), but Alien (N), β1Tubulin (O), and Stripe (P) are not. The *stripe* enhancer trap clearly shows the two rows of cells that make up the ventral attachments of the DPM. DPM da, dorsal attachment of DPM; DPM va, ventral attachment of DPM.

cephalic muscles (GOUBEAUD *et al.* 1996). Although the identities of the muscles involved have not been determined, it is most likely that the cells attach to the dorsal mouthpart muscles, since this pair of muscles extends dorsolaterally from the wall of the pharynx to the epidermis (CAMPOS-ORTEGA and HARTENSTEIN 1997). The level of resolution of STV localization was insufficient to reveal whether or not *stv* is expressed in tendon cells that attach to other cephalic muscles, such as the ventral mouthparts muscle.

Other Starvin-expressing tissues: In addition to the distinctive pattern of expression in epidermal tendon cells, *stv* is also expressed in muscles (Figures 5 and 6). A ventral view of the head region revealed the presence of staining for STV in large muscles, a striking difference between the localization of STV and that of Alien, Stripe, and β1Tubulin (Figure 5M). *stv* is not expressed in all muscles, as STV staining was not observed in the dorsal pharyngeal musculature (Figure 5I). However, *stv* does appear to be expressed in all major somatic muscle

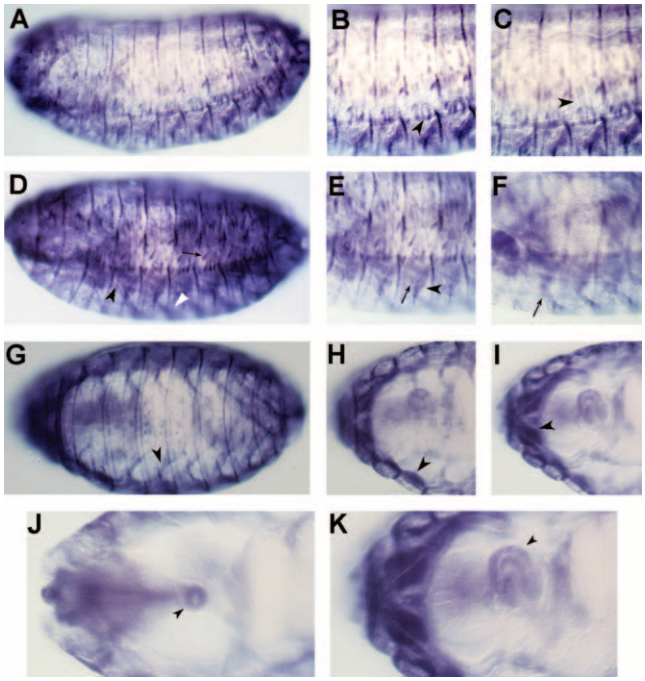

FIGURE 6.—STV is present in somatic muscles and the esophagus. (A) Lateral view of a stage 15 embryo, showing staining in epidermal tendon cells as well as in muscles. B and C are higher magnification views of A in different focal planes. Arrowheads indicate ventral attachments of the lateral transverse muscles (LT1–3). The comparison between B and C suggests that STV is present in both LT muscles and their attachment cells. (D) Lateral view of a stage 16 embryo showing lateral transverse muscles (arrow), ventral oblique muscles (white arrowhead), and a cluster of ventral longitudinal, ventral oblique, and ventral acute muscles (black arrowhead). (E and F) Higher magnification views of D in different focal planes showing ventral olique muscles (arrow) and ventral acute muscles (arrowhead). (G) Ventral view of a stage 16 embryo, showing strong staining for STV in the ventral oblique muscles (VO4–6; arrowhead). (H and I) Higher magnification views of G in different focal planes. The short bars of staining perpendicular to the cuticle represent epidermal tendon cells, while the extended parallel staining is in the muscles. The arrowhead in H indicates very strong staining in longitudinal muscles of T3, which most likely represents ventral intersegmental muscle 5 (VIS5) in combination with the ventral longitudinal muscles. There is also very strong staining in muscles of the first and second thoracic segments. The arrowhead in I indicates muscles in the VIS muscles of the first thoracic segment and possibly the ventral pharyngeal muscles. (J) Dorsal view of the head region of a stage 16 embryo. Staining is observed in a ring structure that is part of the proventriculus (arrowhead). (K) Higher magnification of I showing expression in the tubular esophagus (arrowhead).

groups (Figure 6). Specifically, STV was observed in the ventral oblique muscles, the dense ventral lateral clusters, the lateral transverse muscles, and the ventral intersegmental muscles. Significantly, given the mutant phenotype described below, STV localization was observed to be associated with the esophagus and related junctions, notably the proventriculus (Figure 6, J and K).

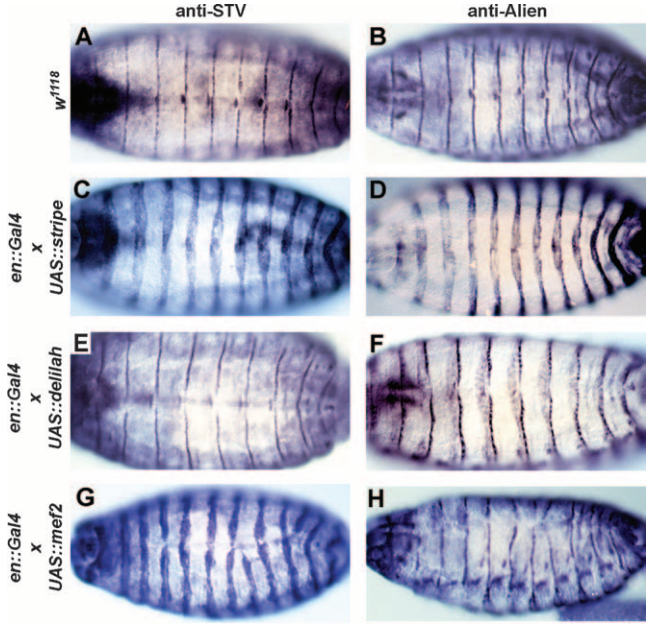

FIGURE 7.—Ectopic expression of *stripe* and *mef2*, but not *delilah*, induces STV. All embryos shown are at stage 16 and viewed dorsally or dorso-laterally. A, C, E, and G are stained with anti-STV and B, D, F, H are stained with anti-Alien. (A and B) w^{1118} control embryos. (C and D) *enGAL4; UASstripe* embryos. (E and F) *enGAL4; UASdelilah* embryos. (G and H) *enGAL4; UASmef2* embryos. STV is clearly induced by ectopic *stripe* (C), but not by ectopic *delilah* (E). Ectopic *mef2* is also sufficient to induce ectopic STV in the ectoderm (G). The irregularity of engrailed domains in the *enGAL4; UASmef2* embryos is due to ectopic *mef2* affecting the patterning of the epidermis and disrupting dorsal closure. Ectopic alien expression is not induced in an *enGAL4; UASmef2* embryo (H), showing that the ectopic induction of *stv* by *mef2* is not a consequence of induction of ectopic tendon cells.

***stv* expression is induced by the *stripe* and *mef2* transcriptional regulatory pathways:** *stripe* function is necessary and sufficient for the epidermal tendon cell fate (LEE *et al.* 1995; FROMMER *et al.* 1996; BECKER *et al.* 1997). Two *stripe* transcripts are known: *stripe* a, which encodes a 1180-amino-acid protein, and *stripe* b, which encodes a 906-amino-acid protein, consisting of the carboxyl 906 residues encoded by *stripe* a. Both isoforms include the early growth response 1 and 2 (EGR)-like triple zinc-finger domain (FROMMER *et al.* 1996). *stripe* b is expressed earlier and more generally, but the final expression pattern is a combination of both transcripts (FROMMER *et al.* 1996).

Ectopic expression of *stripe* b can induce ectopic expression of *kakapo* (*kak*), *delilah* (*dei*), *alien*, and β*1Tubulin* (BECKER *et al.* 1997; VORBRÜGGEN and JÄCKLE 1997). As *stv* is also expressed in the tendon cells, we tested whether ectopic expression of *stv* is also induced by *stripe*. Embryos expressing *stripe* b in the pattern of *engrailed*, utilizing an *en::GAL4 UAS::str* ectopic expression system (BRAND and PERRIMON 1993; BECKER *et al.* 1997), showed ectopic *stv* expression identical to that seen for *alien* (Figure 7, A–D). Using the *24B GAL4* mesoderm-specific driver to express

TABLE 1

***stv* mutant larvae display delayed or arrested growth**

	stv^1/stv^2						stv^2/stv^3						stv^1/stv^3					
	m^-z^+			m^-z^-			m^-z^+			m^-z^-			m^-z^+			m^-z^-		
Days	L1	L2	L3	L1	L2	L3	L1	L2	L3	L1	L2	L3	L1	L2	L3	L1	L2	L3
1	8	24	0	38	0	0	4	26	0	25	0	0	5	45	0	13	26	0
2	0	2	22	14	6	0	0	7	19	9	2	0	0	11	37	9	24	5
3	0	0	21	5	3	1	0	0	25	1	3	1	0	2	42	4	16	18

Larvae were separated into m^-z^+ and m^-z^- classes by the presence or absence, respectively, of GFP fluorescence and allowed to continue to develop on yeast paste. The numbers of live first, second, and third instar larvae were counted at ~1, 2, and 3 days after hatching. Larval instars were distinguished by the size and structure of the mouth-hook apparatus and the structure of the posterior spiracles.

stripe in the muscles (Brand and Perrimon 1993) did not result in ectopic expression of *stv* or *alien* (data not shown), consistent with the previous demonstration that ectopic *stripe* expression cannot induce expression of *kak*, *dei*, *alien*, or β*1Tubulin* in the mesoderm (Vorbrüggen and Jäckle 1997).

dei, which also encodes a transcription factor, is known to be downstream of *stripe* function (Becker *et al.* 1997; Vorbrüggen and Jäckle 1997). DEI is therefore a candidate activator of genes that are known to be downstream of *stripe*, but not known to be direct targets. Ectopic expression of *dei* in the epidermis, driven by the *en::Gal4* driver, induced ectopic *alien* but not *stv* expression (Figure 7, E and F). Thus, *alien* is induced by both *stripe* and *dei*, while *stv* is induced by *stripe* but not by *dei*. It is not known whether *stv* is a direct or an indirect target of *stripe*.

The transcription factor MEF2 is known to be required for the expression of numerous somatic muscle genes. *mef2* expression in the epidermis is known to induce expression of β*3Tubulin*, *nautilus* (*nau*), and *myospheroid* (*mys*; Lin *et al.* 1997). Ectopic STV was induced when *UAS::mef2* (Bour *et al.* 1995) was expressed in the epidermis using the *en::Gal4* or *69B Gal4* drivers (Figure 7G and data not shown). In contrast, Alien expression is only mildly disrupted by *en::Gal4* and *69B Gal4*-induced expression of *mef2* (Figure 7H and data not shown), indicating that the induction of *stv* by *mef2* is not a secondary consequence of an ectopic induction of tendon cell fates.

Generation and analysis of *starvin* mutations: *l(3)00543* is a semilethal allele caused by the insertion of a *P* element within the *stv* transcription unit, although not within the protein-coding sequences. This allele was considered likely to be hypomorphic, so we took two approaches, imprecise *P*-element excision and EMS mutagenesis, to generate amorphic *stv* alleles. Multiple *P*-element reversion strains that exhibited complete lethality were generated and shown by Southern blot analysis to be deletions of regions of *stv*. Two examples are shown diagrammatically in Figure 1B. Imprecise *P*-element excision is not a reliable method of inducing specific null mutations, as deletions may not result in null alleles or may remove functionally unrelated flanking loci. For this reason a screen for EMS-induced mutations that are lethal when *trans*-heterozygous with one of the P reversion stocks, *Df(3L)stv3c*, was carried out.

Four alleles, stv^1, stv^2, stv^3, and stv^4, were generated. stv^1, stv^2, and stv^3 are homozygous and *trans*-heterozygous lethal, while stv^4 is homozygous semilethal. stv^4 is lethal in combination with stv^1 and stv^3, but 20% viable when *trans*-heterozygous with stv^2. The alleles do not form a simple severity series, as stv^1/stv^3 individuals exhibit a milder larval phenotype than stv^1/stv^2 individuals do (see below). The allelic strengths may best be represented as $stv^1 > stv^3 \approx stv^2 > stv^4$. Sequence analysis revealed that stv^1 carries a nonsense mutation, which would result in a truncated protein of 209 aa (23 kDa), one-third the size of wild-type STV (Figure 1) and lacking the BAG domain. Although the molecular lesions in the other alleles were not determined, anti-STV staining could not be detected in stv^1, stv^2, and stv^3 *trans*-heterozygous mutant embryos (data not shown). We conclude that these EMS-induced alleles correspond to mutations in the CG32130/*starvin* gene.

Although we did not observe any STV protein that was deposited maternally, we avoided complications from any possible maternal contribution by generating germline clone maternal mutant embryos using the FLP/FRT Ovo^D method developed by Chou and Perrimon (1996). The germline clone females were crossed to males heterozygous for stv^1. *stv* mutant homozygotes were found to die during the first larval instar. While the number of newly hatched first instar larvae was the expected ratio of 1:1 homozygote:heterozygote, very few homozygous mutant second instar larvae were observed (Table 1). The time of lethality was further examined by separating newly hatched germline clone homozygous and heterozygous larvae using the GFP fluorescence of a marker on the balancer chromosome of the heterozygote. Heterozygotes followed wild-type developmental

timing, with a first molt occurring ~24 hr after hatching and a second at ~48 hr (Table 1). In contrast, *stv*^{1}/*stv*^{2} germline clone mutants could remain as first instars for ≥3 days (Table 1). Only a minority of *stv*^{1}/*stv*^{2} m^{-}z^{-} mutants reached the second larval instar, and these took at least twice as long to do so after hatching, relative to their heterozygous siblings.

***stv* mutant larvae exhibit a severe feeding disability:** One explanation for the failure of the *stv* larvae to grow, or to do so only slowly, is that they may not have been able to feed (see, for example, Zinke *et al.* 1999). Uptake of food can be tested by feeding larvae yeast paste containing bromophenol blue, which acts as a nondigestible dye that is visible in the foregut and midgut (Dubreuil *et al.* 1998). Newly hatched progeny of germline clone crosses were sorted into m^{-}z^{+} and m^{-}z^{-} classes by the presence or absence, respectively, of GFP fluorescence and then allowed to develop on grape agar plates supplemented with yeast paste containing bromophenol blue. *stv*^{1}/*stv*^{2} and *stv*^{2}/*stv*^{3} larvae demonstrated severely reduced or no detectable food uptake, as observed by a minimal amount or absence of bromophenol blue visible in the gut (Figure 8, A–E). Larvae that showed no blue food in the gut failed to grow above hatching size (Figure 8, C and D), although some were observed to live for at least 4 days after hatching. Larvae that showed some food uptake grew from hatching size, but the amount of growth was minimal compared to heterozygous siblings (Figure 8, B and E). The majority of heterozygous larvae increased their weight many times over and molted to second instars ~1 day after hatching. In contrast, all m^{-}z^{-} larvae were still in the first instar (Table 1). Two days after hatching, the majority of heterozygous larvae had undergone the second molt, with no first instars observed, and by 3 days all heterozygous larvae had entered the third larval instar. A minority of m^{-}z^{-} larvae underwent the first molt after 2 days, as determined by mouth-hook size and structure of posterior spiracles, but these larvae were smaller than normal at the second molt (Table 1). By 3 days, rare m^{-}z^{-} mutant third instar larvae were observed (Table 1). These failed to pupate, and in some instances were observed alive 10 days after hatching, grown since molting, but still far smaller than wild-type wandering third instars. However, the majority of *stv* mutant larvae did not develop beyond first instar stage and died well short of reaching wild-type size. The commonly observed size difference between m^{-}z^{-} and m^{-}z^{+} larvae is shown in Figure 8. We also examined the phenotype of zygotic *trans*-heterozygous mutant combinations and found the same slow-growth phenotype and an inability to ingest bromophenol-stained yeast paste, consistent with the absence of observable maternal *stv* product.

In contrast to the severely compromised feeding phenotype and associated stunted growth rate of larvae of the allele combinations *stv*^{1}/*stv*^{2} and *stv*^{2}/*stv*^{3}, the development of *stv*^{1}/*stv*^{3} larvae was only slightly retarded.

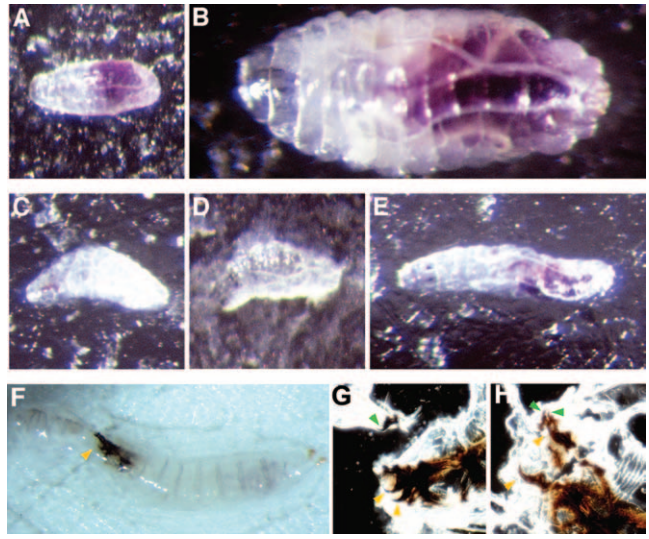

Figure 8.—*stv* mutants have feeding and molting disabilities. (A and B) *stv*^{1}/*TM6B, Tb* germline clone-derived zygotically rescued (m^{-}z^{+}) larvae. (C–E) *stv*^{1}/*stv*^{2} maternal zygotic mutant (m^{-}z^{-}) larvae. (F and G) *stv*^{1}/*stv*^{3} m^{-}z^{-} larvae. All larvae were placed on bromophenol-blue-containing yeast paste <2 hr after hatching. (A and C) Approximately 8 hr after hatching, mutant and zygotically rescued larvae are of a comparable size, although blue food can be seen in the gut of the latter but not the former. (B) By ~48 hr after hatching, this zygotically rescued larva has grown substantially and completed the first molt, while others progress through the second molt (not shown). (D) In contrast, a *stv*^{1}/*stv*^{2} mutant larva, shown at the same magnification as the heterozygous larva in B, has not grown at all. (E) In contrast to D, this larva has doubled in length since hatching, and some blue dye is visible. However, the size increase is minor compared with the zygotically rescued larva of the same age (B), and no molts have occurred. All larvae are shown at the same magnification. (F–H) A hypomorphic allelic combination does not result in feeding difficulties, but a significant proportion of larvae become stuck at the second molt. (F) An example of a *stv*^{1}/*stv*^{3} larva (m^{-}z^{-}) that has failed to molt correctly between the second and third larval instar. This larva has managed to free itself of its old cuticle, but the cuticle remains attached to the mouth-hook apparatus (arrowhead). (G) Larva shown in F squashed between two microscope slides to visualize the mouth hooks. Both the smaller second instar mouth hooks (green arrowheads) and the third instar mouth hooks (red arrowheads) can be seen, indicating that the cuticle remained attached because the mouth hooks have not resolved. (H) Squash of a second larva, which failed to separate the new and old cuticles. Again, both second and third instar mouth hooks can be seen (green and yellow arrowheads, respectively).

Three days after hatching, when virtually all heterozygous larvae were in the third instar, only a small proportion of m^{-}z^{-} larvae remained arrested in the first larval instar, and the remainder were approximately equally divided between the second and third larval instars (Table 1). However, a striking phenotype seen in a proportion of *stv*^{1}/*stv*^{3} larvae was the failure of second instar and third instar mouth hooks to separate, preventing completion of the second molt (Figure 8, F–H, and data not shown).

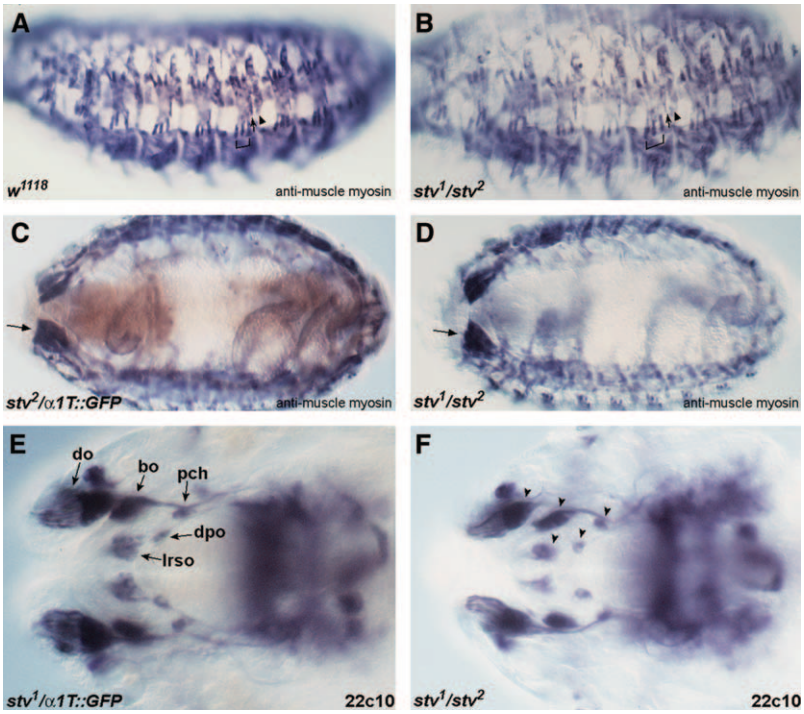

FIGURE 9.—Muscle defects are not evident in *stv* mutants, and head involution proceeds normally. (A–D) Muscle myosin was detected with antimuscle myosin (blue/black). Light brown staining in A, C, and E is anti-GFP to distinguish zygotically rescued embryos. (A) Lateral view of a stage 16 w^{1118} embryo (shown instead of a $m^{-}z^{+}$ embryo to show the wild-type pattern of lateral muscles in the absence of anti-GFP staining). Arrowhead indicates muscle DT1, arrow indicates LT4, and LT1–3 are bracketed. (B) Lateral view of a S16 stv^{1}/stv^{2} $m^{-}z^{-}$ embryo. Symbols as in A. The muscle pattern appears normal. (C) Ventral view of a S16 $stv^{2}/TM6B$, $\alpha 1Tubulin::GFP$ $m^{-}z^{+}$ embryo. Arrow indicates the large VIS muscles. (D) Ventral view of a S16 stv^{1}/stv^{2} $m^{-}z^{-}$ embryo. Arrow indicates the large VIS muscles. The muscle pattern appears normal. (E and F) Mab 22C10 staining of stage 16 embryos. (E) Dorsal view of the head region of a S16 $stv^{1}/TM6B$, $\alpha 1Tubulin::GFP$ $m^{-}z^{+}$ embryo. *do*, dorsal organ; *bo*, Bolwig's organ; *pch*, dorsal pharyngeal chordotonal organ; *dpo*, dorsal pharyngeal organ; *lrso*, labral sensory complex. Before head involution, *lrso* and *dpo* extend anteriorly to *do*. (F) Dorsal view of the head region of a S16 stv^{1}/stv^{2} $m^{-}z^{-}$. The relative positions of the sense organs (arrowheads) indicate that head involution has proceeded normally.

Muscle and head involution defects are not evident in *stv* mutant embryos: There are numerous possible behavioral, morphological, and physiological reasons for reduced or absent feeding. Given the expression of *stv* in muscle and tendon cells, the most likely explanation was some type of muscle defect. The most common phenotypes for mutants of genes expressed in epidermal tendon cells are misguidance of muscles (and thus misattachment) and the failure of maintenance of attachment. For example, *stripe* mutant embryos exhibit elongated muscle processes and occasional rounding up of muscles that have broken their attachments (FROMMER *et al.* 1996). Rounding up of muscles is the prominent phenotype of *mys* and *irregular facets* (*if*) mutant embryos (LEPTIN *et al.* 1989; BRABANT and BROWER 1993; BROWN 1994). Muscles of *kak* mutant embryos detach from the epidermis during stage 17 because of a lack of structural integrity of the epidermal cells, which tear in two under the stress of muscle contraction (GREGORY and BROWN 1998; PROKOP *et al.* 1998b). A severe somatic muscle attachment phenotype should also result in embryonic lethality or, at least, larval movement defects. Neither of these was observed in *stv* mutant homozygotes. The tracks left by *stv* mutants did not obviously differ in length or complexity from those of wild-type larvae. Like normal larvae, *stv* mutant larvae were found to converge on yeast paste and mouth-hook movements were indistinguishable from those of normal larvae while feeding (data not shown). The gross feeding behavior of *stv* mutant larvae therefore appeared to be normal.

To further test whether muscle structure was affected, we used antimuscle myosin to visualize somatic muscles in *stv* mutant embryos (Figure 9, A–D). Germline clone mutant embryos, lacking both maternal and zygotic *stv* products, exhibited no muscle abnormalities. All major muscle groups were observed to be present and showed no sign of disorganization.

One known cause of larval feeding failure is incomplete head involution during embryogenesis. For example, mutants specific for the cytoskeletal isoform of tropomyosin die as first instar larvae because they cannot feed (TETZLAFF *et al.* 1996). These mutants are normal until stage 16 of embryogenesis, but head involution fails to occur, and the hatching larvae have a protruding pharyngeal mass (TETZLAFF *et al.* 1996). Progression of head involution can be followed by the relative positions of the head sensory organs. Before head involution occurs, the labral sensory complex (lrso) and dorsal pharyngeal organ (dpo) are positioned the farthest anteriorly, such that the lrso is anterior to the dorsal organ (do) (CAMPOS-ORTEGA and HARTENSTEIN 1997). Staining with monoclonal antibody 22C10 showed that the relative positions of the sense organs in the head are the same in late mutant and heterozygous larvae (Figure 9, E and F), indicating that head involution occurred normally in *stv* mutant larvae.

We conclude, therefore, that feeding is compromised in *stv* mutant larvae not as a consequence of a more general defect, but because of something that specifically affects the ingestion of food.

DISCUSSION

We report here a developmental and genetic characterization of the Drosophila gene *stv*. The derived amino acid sequence of STV revealed significant similarity to the BAG family of genes. The region of similarity in STV extends almost 80 aa and includes the 47-aa BAG domain originally defined by Takayama *et al.* (1999). The BAG family is an important gene family implicated in a variety of biological roles, most often through their role as Hsp70 and Hsc70 cochaperones.

stv is expressed in a highly tissue-specific manner in epidermal muscle attachment cells and in somatic muscles, as well as in parts of the esophagus or associated tissues. It should be noted that the Berkeley *Drosophila* Genome Project *in situ* data (http://www.fruitfly.org/cgi-bin/ex/insitu.pl) show midgut expression that we did not observe. We may have missed this expression because it is transient or because of translational regulation or because of limited antibody penetration.

Very few genes are expressed specifically in both epidermal muscle attachment cells and associated somatic muscles. *myospheroid* (encoding the βPS integrin subunit) is expressed in both tissues, and βPS integrin localizes to the membrane, concentrated at the sites of muscle-epidermal attachment (Brown *et al.* 1993). The second gene known to be expressed in both muscles and their attachments is *held out wings* (*how*), which encodes an RNA-binding domain protein that regulates tendon cell differentiation (Nabel-Rosen *et al.* 2002 and references therein). In contrast to the localization of STV, expression of *how* begins early, zygotic message being observed in the mesoderm from the beginning of gastrulation. *how* remains expressed in cells that will form the somatic, visceral, and cardiac muscles. During dorsal closure, expression also becomes apparent in the epidermal muscle attachment cells. Levels of HOW remain highest in the cardiac muscles (dorsal vessel) and epidermal muscle attachment cells (Baehrecke 1997; Fyrberg *et al.* 1997; Lo and Frasch 1997; Zaffran *et al.* 1997). The latter pattern of HOW localization is similar to that of STV, although no appreciable levels of STV are detected in the dorsal vessel. Thus, STV has a unique distribution, being present in fewer tissues than HOW and more generally localized within the cell than βPS.

The accumulation of STV in epidermal muscle attachment cells is most similar to the accumulation of β1Tubulin and Delilah, which are first observed in weak intersegmental stripes during stage 13, which increase in intensity during stages 15 and 16 (Armand *et al.* 1994; Buttgereit 1996; Yarnitzky *et al.* 1997). In contrast, *kak*, *alien*, and *stripe* begin to be expressed earlier, at stage 11, and always at their final intensity (Lee *et al.* 1995; Frommer *et al.* 1996; Goubeaud *et al.* 1996; Strumpf and Volk 1998). *stv* regulation falls within previously characterized muscle and tendon transcriptional regulatory pathways. *stv* is downstream of *stripe* function in the epidermis, but not of *delilah*. In contrast, expression of *alien* was found to be downstream of both *stripe* and *delilah*. In somatic muscle, *stv* appears to be under the regulation of the transcription factor *mef2*.

stv mutant individuals lack the ability to take up food and die most often as first or, occasionally, as second or third instar larvae. The survival for days after hatching, even of larvae that apparently fail to eat at all, is consistent with previously observed rates of survival under starvation conditions. Larvae hatched onto PBS solution live for 2–3 days, and on 20% sucrose in PBS for ~8 days (Britton and Edgar 1998; B. Edgar, personal communication). In both instances, larvae remain small and arrested in the first larval instar. The delayed development and reduced growth of *stv* mutant larvae is therefore most likely due to a severely reduced uptake of nutrients necessary for growth.

We were unable to determine the precise cause of the feeding impairment. The localization of STV to epidermal tendon cells and somatic muscles suggests a role in muscle development, attachment, or function, but morphological defects in muscle structures were not observed. Consistent with this, *stv* mutant larvae hatch, crawl around apparently normally, and exhibit normal mouth-hook movements. It is possible that a specific muscle involved in control of the esophagus is particularly sensitive to disruption by the absence of *stv* function, manifesting as a phenotype that is more specific than would be predicted from the broad tendon and muscle cell expression of *stv*. Alternatively, defects in the foregut, proventriculus, or gastric cecum can result in feeding defects. However, again, no obvious defects were observed in the morphology of these structures in *stv* mutant larvae. The gross anatomy of the muscles and gut of late *stv* mutant embryos appeared normal, but subtle changes may have been missed in our analysis. Alternatively, *stv* may not be required for tissue structure, but may be required for proper physiological function of muscle or esophageal structures. Consistent with this, STV appears in muscles only after attachment, so it is likely to have a role in the later aspects of muscle maturation or function. Subtle changes in muscle function may also explain the stv^{1}/stv^{3} mutant larvae that die at the molt between the second and third larval instars from failure of the old and new sets of mouth hooks to separate, as the muscles responsible for moving the mouth hooks are thought to detach from the set to be discarded and to establish connections to the new mouth hooks (Crossley 1978).

The functions of mammalian BAG-domain proteins shed little light on the *stv* mutant phenotype. The BAG domain of STV is most similar to those of human BAG-4, which is also referred to as SODD (*s*uppressor *o*f the *d*eath *d*omain), human BAG-3, and one of the human BAG-5 BAG domains. BAG-4 is a 457-aa binding partner

of *t*umor *n*ecrosis *f*actor *r*eceptor 1 (TNF-R1) and death receptor 3 (Jiang *et al.* 1999; Miki and Eddy 2002) and, like other human BAG-domain proteins, also interacts with Bcl2. BAG-4/SODD appears to have roles similar to other human BAG-domain proteins in acting in an antipapoptotic manner, for example, suppressing apoptosis when overexpressed in pancreated cancer cells (Liao *et al.* 2001) and suppressing TNF-induced apoptosis (Miki and Eddy 2002). BAG-3 forms a ternary complex with Hsc70 and phospholipase Cγ (PLCγ) in response to EGF. PLCγ is contacted by BAG-3 through a domain comprising multiple PXXP motifs leaving the BAG domain free to contact Hsp70 (Doong *et al.* 2000). BAG-5 also exhibits Hsp70-binding ability, along with an ability to interact directly with parkin, an E3 ubiquitin ligase frequently mutated in early-onset Parkinson's disease (Kalia *et al.* 2004). In this case, BAG-5 inhibits parkin E3 ubiquitin ligase activity and Hsp70-mediated refolding of misfolded proteins and, in contrast to other BAG-domain proteins, acts as an antisurvival factor in dopaminergic neurons (Kalia *et al.* 2004). Consequently, although we can be confident that STV will act as an Hsp70-family chaperone and, most likely, bind to other proteins to modify their function, the potential targets are numerous, making their cellular and developmental roles impossible to predict. Curiously, some mutant alleles of *Actin88F* induce heat-shock proteins at normal temperatures. In these mutants, heat-shock proteins are bound to the myofiber, suggesting that they stabilize the mutant Actin forms (reviewed by Bernstein *et al.* (1993). However, the predominantly normal function of the muscles in *stv* mutant embryos suggests that if such a role exists for STV, it must be relatively minor.

Irrespective of the difficulty in establishing a developmental or physiological explanation for the *stv* mutant feeding phenotype, our analysis has yielded several important observations that shed new light onto the function of the BAG-family genes. The developmental specificity, larval lethality, and feeding and molting phenotypes raise the possibility that one or more of the BAG-family genes plays developmentally specific roles during mammalian development.

We thank B. Bour, D. Buttgereit, A. Michelson, A. Paululat, and T. Volk for the gifts of fly strains and antibodies. This work was funded by the Australian Research Council and the National Health and Medical Research Council of Australia. M. Coulson was supported by an Australian Postgraduate Research Award and S. Robert was supported by a University of Adelaide Faculty of Science Scholarship.

LITERATURE CITED

Alberti, S., C. Esser and J. Höhfeld, 2003 BAG-1—a nucleotide exchange factor of Hsc70 with multiple cellular functions. Cell Stress Chaperones **8:** 225–231.

Antoku, K., R. S. Maser, W. J. Scully, Jr., S. M. Delach and D. E. Jonhson, 2001 Isolation of Bcl-2 binding proteins that exhibit homology with BAG-1 and suppressor of death domains protein. Biochem. Biophys. Res. Commun. **286:** 1003–1010.

Armand, P., A. C. Knapp, A. J. Hirsch, E. F. Wiechaus and M. D. Cole, 1994 A novel basic helix-loop-helix protein is expressed in muscle attachment sites of the *Drosophila* epidermis. Mol. Cell. Biol. **14:** 4145–4154.

Baehrecke, E. H., 1997 *who* encodes a KH RNA binding protein that functions in muscle development. Development **124:** 1323–1332.

Bardelli, A., P. Longati, D. Albero, S. Goruppi, C. Schneider *et al.*, 1996 HGF receptor associates with the anti-apoptotic protein BAG-1 and prevents cell death. EMBO J. **15:** 6205–6212.

Becker, S., G. Pasca, D. Strumpf, L. Min and T. Volk, 1997 Reciprocal signaling between *Drosophila* epidermal muscle attachment cells and their corresponding muscles. Development **124:** 2615–2622.

Bernstein, S. I., P. T. O'Donnell and R. M. Cripps, 1993 Molecular genetic analysis of muscle development, structure, and function in *Drosophila*. Int. Rev. Cytol. **143:** 63–152.

Bour, B. A., M. A. O'Brien, W. L. Lockwood, E. S. Goldstein, R. Bodmer *et al.*, 1995 *Drosophila* MEF2, a transcription factor that is essential for myogenesis. Genes Dev. **9:** 730–741.

Brabant, M. C., and D. L. Brower, 1993 PS2 integrin requirements in *Drosophila* embryo and wing morphogenesis. Dev. Biol. **157:** 49–59.

Brand, A. H., and N. Perrimon, 1993 Targeted gene expression as a means of altering cell fates and generating dominant phenotypes. Development **118:** 401–415.

Briknarova, K., S. Takayama, L. Brive, M. L. Havert, D. A. Knee *et al.*, 2001 Structural analysis of BAG1 cochaperone and its interactions with Hsc70 heat shock protein. Nat. Struct. Biol. **8:** 349–352.

Briknarova, K., S. Takayama, S. Homma, K. Baker, E. Cabezas *et al.*, 2002 BAG4/SODD protein contains a short BAG domain. J. Biol. Chem. **277:** 31172–31178.

Britton, J. S., and B. A. Edgar, 1998 Environmental control of the cell cycle in *Drosophila*: nutrition activates mitotic and endoreplicative cells by distinct mechanisms. Development **125:** 2149–2158.

Brockmann, C., D. Leitner, D. Labudde, A. Diehl, V. Sievert *et al.*, 2004 The solution structure of the SODD BAG domain reveals additional electrostatic interactions in the HSP70 complexes of SODD subfamily BAG domains. FEBS Lett. **558:** 101–106.

Brown, N. H., 1994 Null mutations in the αPS2 and βPS integrin subunit genes have distinct phenotypes. Development **120:** 1221–1231.

Brown, N. H., and T. C. Kafatos, 1988 Functional cDNA libraries from *Drosophila* embryos. J. Mol. Biol. **203:** 425–437.

Brown, N. H., J. W. Bloor, O. Dunin-Borkowski and M. D. Martin-Bermudo, 1993 Integrins and morphogenesis. Development **1993**(Suppl.): 177–183.

Buttgereit, D., 1996 Transcription of the β1 tubulin (βTub56D) gene in apodemes is strictly dependent on muscle insertion during embryogenesis in *Drosophila melanogaster*. Eur. J. Cell Biol. **71:** 183–191.

Campos-Ortega, J. A., and V. Hartenstein, 1997 *The Embryonic Development of Drosophila melanogaster*. Springer-Verlag, Berlin.

Chou, T.-B., and N. Perrimon, 1996 The autosomal FLP-DFS technique for generating germline mosaics in *Drosophila melanogaster*. Genetics **144:** 1673–1679.

Crossley, A. C., 1978 The morphology and development of the *Drosophila* musculature system, pp. 499–560 in *The Genetics and Biology of Drosophila*, edited by M. Ashburner and T. R. F. Wright. Academic Press, London.

Doong, H., J. Price, Y. S. Kim, C. Gasbarre, J. Probst *et al.*, 2000 CAIR-1/BAG-3 forms an EGF-regulated ternary complex with phospholipase C-gamma and Hsp70/Hsc70. Oncogene **19:** 4385–4395.

Doong, H., A. Vrailas and E. C. Kohn, 2002 What's in the 'BAG'?—a functional domain analysis of the BAG family proteins. Cancer Lett. **188:** 25–32.

Dubreuil, R. R., J. Frankel, P. Wang, J. Howrylak, M. Kappil *et al.*, 1998 Mutations of α spectrin and *labial* block cuprophilic cell differentiation and acid secretion in the middle midgut of *Drosophila* larvae. Dev. Biol. **194:** 1–11.

FlyBase, 1999 The FlyBase database of the Drosophila genome projects and community literature. Nucleic Acids Res. **27:** 85–88 (http://flybase.bio.indiana.edu).

Froesch, B. A., S. Takayama and J. C. Reed, 1998 BAG-1L protein enhances androgen receptor function. J. Biol. Chem. **273:** 11660–11666.

Frommer, G., G. Vorbrüggen, G. Pasca, H. Jäckle and T. Volk, 1996 Epidermal egr-like zinc finger protein of Drosophila participates in myotube guidance. EMBO J. **15:** 1642–1649.

Fyrberg, C., J. Becker, P. Barthmaier, J. Mahaffey and E. Fyrberg, 1997 A *Drosophila* muscle-specific gene related to the mouse *quaking* locus. Gene **197:** 315–323.

Gassler, C. S., T. Wiederkehr, D. Brehmer, B. Bukau and M. P. Mayer, 2001 Bag-1M accelerates nucleotide release for human Hsc70 and Hsp70 and can act concentration-dependent as positive and negative cofactor. J. Biol. Chem. **276:** 32538–32544.

Gebauer, M., M. Zeiner and U. Gehring, 1997 Proteins interacting with the molecular chaperone hsp70/hsc70: physical associations and effects on refolding activity. FEBS Lett. **417:** 109–113.

Gehring, U., 2004 Biological activities of HAP46/BAG-1. EMBO Rep. **5:** 148–153.

Goubeaud, A., S. Knirr, R. Renkawitz-Pohl and A. Paululat, 1996 The *Drosophila* gene *alien* is expressed in the muscle attachment sites during embryogenesis and encodes a protein highly conserved between plants, *Drosophila* and vertebrates. Mech. Dev. **57:** 59–68.

Gregory, S. L., and N. H. Brown, 1998 *kakapo*, a gene required for adhesion between and within cell layers in *Drosophila*, encodes a large cytoskeletal linker protein related to plectin and dystrophin. J. Cell Biol. **143:** 1271–1282.

Grigliatti, T., 1986 Mutagenesis, pp. 55–83 in *Drosophila: A Practical Approach*, edited by D. B. Roberts. IRL Press, Oxford.

Höhfeld, J., 1998 Regulation of the heat shock conjugate Hsc70 in the mammalian cell: the characterization of the anti-apoptotic protein BAG-1 provides novel insights. Biol. Chem. **379:** 269–274.

Höhfeld, J., and S. Jentsch, 1997 GrpE-like regulation of the Hsc70 chaperone by the anti-apoptotic protein BAG-1. EMBO J. **16:** 6209–6216.

Hung, W. J., R. S. Roberson, J. Taft and D. Y. Wu, 2003 Human BAG-1 proteins bind to the cellular stress response protein GADD34 and interfere with GADD34 functions. Mol. Cell. Biol. **23:** 3477–3486.

Jiang, Y., J. D. Woronicz, W. Liu and D. V. Goeddel, 1999 Prevention of constitutive TNF receptor 1 signaling by silencer of death domains. Science **283:** 543–546.

Kalia, S. K., S. Lee, P. D. Smith, L. Liu, S. J. Crocker *et al.*, 2004 BAG5 inhibits Parkin and enhances dopaminergic neuron degeneration. Neuron **44:** 931–945.

Kiehart, D. P., and R. Feghali, 1986 Cytoplasmic myosin from *Drosophila melanogaster*. J. Cell Biol. **103:** 1517–1525.

Kullmann, M., J. Schneikert, J. Moll, S. Heck, M. Zeiner *et al.*, 1998 RAP46 is a negative regulator of glucocorticoid receptor action and hormone-induced apoptosis. J. Biol. Chem. **273:** 14620–14625.

Lee, J. C., K. VijayRaghavan, S. E. Celniker and M. A. Tanouye, 1995 Identification of a *Drosophila* muscle development gene with structural homology to mammalian early growth response transcription factors. Proc. Natl. Acad. Sci. USA **92:** 10344–10348.

Leptin, M., T. Bogaert, R. Lehmann and M. Wilcox, 1989 The function of PS integrins during *Drosophila* embryogenesis. Cell **56:** 401–408.

Liao, Q., F. Ozawa, H. Friess, A. Zimmermann, S. Takayama *et al.*, 2001 The anti-apoptotic protein BAG-3 is overexpressed in pancreatic cancer and induced by heat stress in pancreatic cancer cell lines. FEBS Lett. **503:** 151–157.

Lin, M.-H., B. A. Bour, S. M. Abmayr and R. V. Storti, 1997 Ectopic expression of MEF2 in the epidermis induces epidermal expression of muscle genes and abnormal muscle development in *Drosophila*. Dev. Biol. **182:** 240–255.

Liu, R., S. Takayama, Y. Zheng, B. Froesch, G. Q. Chen *et al.*, 1998 Interaction of BAG-1 with retinoic acid receptor and its inhibition of retinoic acid-induced apoptosis in cancer cells. J. Biol. Chem. **273:** 16985–16992.

Lo, P. C. H., and M. Frasch, 1997 A novel KH-domain protein mediates cell adhesion processes in *Drosophila*. Dev. Biol. **190:** 241–256.

Manchen, S. T., and A. V. Hubberstey, 2001 Human Scythe contains a functional nuclear localization sequence and remains in the nucleus during staurosporine-induced apoptosis. Biochem. Biophys. Res. Commun. **287:** 1075–1082.

Matsuzawa, S., S. Takayama, B. A. Froesch, J. M. Zapata and J. C. Reed, 1998 p53-inducible human homologue of Drosophila seven in absentia (Siah) inhibits cell growth: suppression by BAG-1. EMBO J. **17:** 2736–2747.

Miki, K., and E. M. Eddy, 2002 Tumor necrosis factor receptor 1 is an ATPase regulated by silencer of death domain. Mol. Cell. Biol. **22:** 2536–2543.

Nabel-Rosen, H., G. Volohonsky, A. Reuveny, R. Zaidel-Bar and T. Volk, 2002 Two isoforms of the Drosophila RNA binding protein, how, act in opposing directions to regulate tendon cell differentiation. Dev. Cell **2:** 183–193.

Prokop, A., J. Uhler, J. Roote and M. Bate, 1998b The *kakapo* mutation affects terminal arborization and central dendritic sprouting of *Drosophila* motorneurons. J. Cell Biol. **143:** 1283–1294.

Robert, S., and R. Saint, 1998 Rapid screening for protein interactors using in vitro translated protein and an expression library. Technical Tips Online (http://www.elsevier.com/locate/tto).

Shatkina, L., S. Mink, H. Rogatsch, H. Klocker, G. Langer *et al.*, 2003 The cochaperone Bag-1L enhances androgen receptor action via interaction with the NH2-terminal region of the receptor. Mol. Cell. Biol. **23:** 7189–7197.

Sondermann, H., C. Scheufler, C. Schneider, J. Hohfeld, F. U. Hartl *et al.*, 2001 Structure of a Bag/Hsc70 complex: convergent functional evolution of Hsp70 nucleotide exchange factors. Science **291:** 1553–1557.

Song, J., M. Takeda and R. I. Morimoto, 2001 Bag1-Hsp70 mediates a physiological stress signalling pathway that regulates Raf-1 /ERK and cell growth. Nat. Cell Biol. **3:** 276–282.

Strumpf, D., and T. Volk, 1998 Kakapo, a novel cytoskeletal-associated protein is essential for the restricted localization of the neuregulin-like factor, Vein, at the muscle-tendon junction site. J. Cell Biol. **143:** 1259–1270.

Symersky, J., Y. Zhang, N. Schormann, S. Li, R. Bunzel *et al.*, 2004 Structural genomics of Caenorhabditis elegans: structure of the BAG domain. Acta Crystallogr. D Biol. Crystallogr. **60:** 1606–1610.

Takayama, S., T. Sato, S. Krajewski, K. Kochel, S. Irie *et al.*, 1995 Cloning and functional analysis of BAG-1: a novel Bcl-2-binding protein with anti-cell death activity. Cell **80:** 279–284.

Takayama, S., D. N. Bimston, S. Matsuzawa, B. C. Freeman, C. Aime-Sempe *et al.*, 1997 BAG-1 modulates the chaperone activity of Hsp70/Hsc70. EMBO J. **16:** 4887–4896.

Takayama, S., Z. Xie and J. C. Reed, 1999 An evolutionarily conserved family of Hsp70/Hsc70 molecular chaperone regulators. J. Biol. Chem. **274:** 781–786.

Tetzlaff, M. T., H. Jäckle and M. J. Pankratz, 1996 Lack of *Drosophila* cytoskeletal tropomyosin affects head morphogenesis and the accumulation of *oskar* mRNA required for germ cell formation. EMBO J. **15:** 1247–1254.

Thress, K., J. Song, R. I. Morimoto and S. Kornbluth, 2001 Reversible inhibition of Hsp70 chaperone function by Scythe and Reaper. EMBO J. **20:** 1033–1041.

Townsend, P. A., A. Stephanou, G. Packham and D. S. Latchman, 2005 BAG-1: a multi-functional pro-survival molecule. Int. J. Biochem. Cell Biol. **37:** 251–259.

Vorbrüggen, G., and H. Jäckle, 1997 Epidermal muscle attachment site-specific target gene expression and interference with myotube guidance in response to ectopic *stripe* expression in the developing *Drosophila* epidermis. Proc. Natl. Acad. Sci. USA **94:** 8608–8611.

Wang, H. G., S. Takayama, U. R. Rapp and J. C. Reed, 1996 Bcl-2 interacting protein, BAG-1, binds to and activates the kinase Raf-1. Proc. Natl. Acad. Sci. USA **93:** 7063–7068.

Yarnitzky, T., L. Min and T. Volk, 1997 The *Drosophila* neuregulin homolog Vein mediates inductive interactions between myotubes and their epidermal attachment cells. Genes Dev. **11:** 2691–2700.

Zaffran, S., M. Astier, D. Gratecos and M. Sémériva, 1997 The *held out wings* (*how*) *Drosophila* gene encodes a putative RNA-binding protein involved in the control of muscular and cardiac activity. Development **124:** 2087–2098.

Zeiner, M., M. Gebauer and U. Gehring, 1997 Mammalian protein RAP46: an interaction partner and modulator of 70kDa heat shock proteins. EMBO J. **16:** 5483–5490.

Zinke, I., C. Kirchner, L. C. Chao, M. T. Tetzlaff and M. J. Pankratz, 1999 Suppression of food intake and growth by amino acids in Drosophila: the role of pumpless, a fat body expressed gene with homology to vertebrate glycine cleavage system. Development **126:** 5275–5284.

Communicating editor: T. C. Kaufman